Colloidal Dispersions of Octadecyl Grafted Silica Spheres in Toluene: A Global Analysis of SANS Contrast Variation and Concentration Dependence Measurements

by

Joachim Kohlbrecher[1]

and

Johan Buitenhuis[2], Gerhard Meier[2] and M. Paul Lettinga[2]

1: SINQ, Paul-Scherrer Institut, 5232Villigen PSI , Switzerland

2: IFF, weiche Materie, Forschungszentrum Jülich, Postfach 1913, 52425 Jülich, Germany

Abstract

In this paper we report measurements of the form factor and the structure factor of a sterically stabilized colloidal dispersion consisting of silica spheres coated with octadecane in toluene by small angle neutron scattering, SANS. The phase diagram of this system shows the liquid-liquid coexistence line and also a jamming transition at higher concentrations, where the jamming line intersects the coexistence line roughly at the critical point. We have performed SANS experiments at a temperature well above the transition temperature and at various volume fractions ϕ, spanning from the very dilute regime (ϕ=0.2%) to the critical concentration (ϕ=16%) and the highly viscous regime (ϕ=39.2%). Except for the very dilute regime, we observe a structure factor $S(q)$ in all other cases. We fitted our data over the whole concentration regime using a global fitting routine with a core-shell model for the form factor $P(q)$, taking into account the structure factor, which we describe with the Robertus model for an adhesive polydisperse core-shell particle. At a volume fraction of ϕ=5% a SANS contrast variation experiment has been performed. From that the product of the volume of the shell and the amount of solvent within the corona of our core-shell particle could be determined.. At the most probable shell thickness of 2.3nm a solvent content of about 50% within the corona was found. Moreover we could conclude that the core is not interpenetrated by solvent molecules. From the contrast variation experiment followed that the structure factor at zero average contrast exhibits a strong q-dependence, which is an effect of an inhomogeneous particle in combination with a size distribution.

I. Introduction

A very successful theory to describe colloidal systems is the so-called hard-sphere theory, in which particles interact only at the closest approach via an infinitely steep pair potential. Here the particle radius is simply set by excluded volume only[1]. In cases where the potential raises not that steep, like a Yukawa type potential[2], the effective hard sphere diameter can be adjusted or equivalently the effective volume fraction. This still allows for a reliable estimation of the equilibrium structure and thermodynamic properties. The situation is getting more complex, if one adds a short range attractive interaction or potential to the hard sphere model. This potential is called a square well potential or specifically the Baxter model for an adhesive hard sphere[3] and is sketched in Fig. 1 schematically. Systems, which can be described with such a potential, show rich phase behaviour, if the attractive part is strong enough. Examples for those systems are sterically stabilized colloids in marginal solvents, which were reported for example by Jansen et al.[4], Edwards et al.[5] and Rouw and de Kruif [6]. The model system we use for our investigations was introduced by de Kruif and Schouten[7] and consists of silica spheres grafted with octadecyl chains in toluene However, also the use of other marginal solvents has been reported [8,9,10].

In toluene at a volume fraction of about ϕ=0.1 a liquid-liquid phase transition is observed, in a very convenient temperature and pressure range. In the case of sterically stabilized colloids the nature of the interaction in the hairy corona of the silica spheres will change with pressure and temperature[7] and a liquid- liquid phase transition will take place. The interaction between spheres is short ranged, therefore we can assume that its relevant length scale is at most as long as the corona thickness, which is in the order of 2nm, as concluded from geometric considerations. Most probably the structure of the corona, and to a lesser extend the silica core, plays a key role in the liquid-liquid phase transition[4]. Knowledge of these features can be obtained from small angle neutron scattering SANS as has been shown in numerous other investigations on core shell particles[11,12,13,14,15], since it can provide us with the desired information by performing contrast variation experiments. However, an unambiguous interpretation of such data is not straight forward. Therefore it is the main objective of this paper to present a most detailed investigation of the equilibrium configuration of our system. The SANS data will-yield structural information on length scales comparable to the size of the spheres used in our experiments, being about 80nm in diameter and its corona thickness Thereby we take advantage of the fact, that the scattering length density of the silica core can be matched by a proper mixture of protonated and deuterated solvent such that only the corona is visible and hence subtle changes there are well detected. Two important features come up while dealing with properties of the corona of a core–shell particle: Its thickness and its possible penetration by solvent molecules. In combination to that the grafting density is important, since both parameters characterize the effective scattering length density, which is essential to know performing a numerical analysis of the scattering data in order to extract the thickness. In this paper we will first characterize our system, i.e. the phase diagram as obtained by "simple" visual inspection, the SANS experiments to determine the form and structure factors and a contrast variation to explore the solution properties in more detail with the aim to learn something about the layer thickness and its penetration by solvent molecules. To this end we will employ a global fit routine, which allows to use fit parameters simultaneously for a whole series of data curves and is thus capable to provide information which would not be possible to obtain from a single curve fit alone. Last but not least we have investigated the volume fraction dependence of the intensity to measure the structure factor and will analyze the data on the basis of various models for $S(q)$ including the Baxter model, thereby using an algorithm for the numerical calculation of the structure factor for a polydisperse system[16]. The paper is organized as follows: In section II we will present the experimental methods used, synthesis, TEM, LS and SANS. In section IIIA we will present the phase diagram leading over to the SANS: Basic formulas are presented in section IIIB, followed by results, first the structure factor, section IIIC, and then the contrast variation, section IIID. We conclude with section IV.

II. Experimental

A. Synthesis and Elemental Analysis

Silica core particles were prepared according to Stöber[17] and then grafted with stearyl alcohol following van Helden[18] to obtain octadecyl chains anchored onto the surface. The dispersion was purified by repeated cycles of centrifugation and redispersion in chloroform and cyclohexane. Stock solutions were prepared by drying the dispersion under a nitrogen flow at about 50°C and immediately followed by redispersing in toluene-h8 and toluene-d8. All further samples were prepared by pipetting from these two stock solutions. The concentration of these solutions was determined by drying a small volume of dispersion to constant weight at 150°C. After storage for some longer time the concentration of the stock solutions was checked.

The volume fraction of the dispersions was obtained from the weight concentration and the density of the particles. The density of the particles was determined from the density of a dispersion with a concentration of 0.665 g/mL. This was done by weighting 10 mL of the dispersion as well as the solvent toluene-h8 in the same measuring flask. Assuming additivity of volumes of solvent and particles, which is a good assumption for these colloidal dispersions, a density of the particles of ρ_p=1.78 g/mL was obtained.

Elemental analysis was performed by the Central Division of Analytical Chemistry (ZCH) of the Forschungszentrum Jülich on a LECO CHNS-932 analyzer. The sample was dried for 24 hours at 50 °C under vacuum. An average carbon content of 9.5 w/w% was obtained, which is attributed to 11.1 w/w% alkyl chains. Assuming additivity of volumes and a density of 0.78 g/mL for the alkyl chains and 2.0 g/mL for the silica a volume fraction of 24.3% of alkyl chains in the particles can be estimated from this weight concentration. This value will be compared to the SANS result later.

B. Sample Characterisation by TEM and LS

We have performed static(SLS) and dynamic(DLS) light scattering as well as transmission electron microscopy (TEM) on our samples. The light scattering was performed on a custom made goniometer, which allows to measure the static and dynamic light scattering in an angular range from θ=30°-120°. The concentration of spheres used for the light scattering experiments was 1g/l. As a result from dynamic light scattering experiments, a single exponential decay of the intensity autocorrelation function and a decay rate proportional to square of the scattering vector is obtained. From that a diffusion coefficient of $D=9.84\times10^{-12}$ m^2/s is calculated which in turn gives a radius of r=39.6nm via the Stokes-Einstein relation. Likewise the radius of the particles can be obtained from a Guinier analysis of the total scattered intensity $I(q)$ as a function of angle. From the slope of the Guinier plot a radius of $(5/3)^{1/2}r_G$ was calculated, which gives r=43nm in fair agreement with the result from the dynamic measurement.

Transmission electron microscopy (TEM) has been performed on a Philips CM200 microscope at a voltage of 200 kV. A drop of 1g/l solution was put on a regular TEM grid and was transmitted after force drying without further masking. In Fig. 2 the histogram of the size distribution obtained from our TEM data is shown. All together 177 particles have been analysed by standard image processing software, resulting in a mean diameter of $<d>$=67nm with a relative standard deviation of σ=0.13. On comparing the average diameter from TEM with the values from LS one has to consider, that TEM is sensitive on the number average diameter of the particles, whereas dynamic light scattering is sensitive to a higher order average, specifically, it measures the 6th moment of the inverse *z*-averaged diameter. Inspection of Fig. 2 shows, that the distribution is asymmetric towards higher diameters. We find different values for d obtained from light scattering and from TEM. For the here obtained standard deviation of σ=0.13 the ratio in diameters according to Thomas[19] should be, d_{LS}/d_{TEM} = 1.22. We find 83/67=1.24, which is in good agreement. A source of uncertainty stems from the fact, that the contrast in TEM from the corona of the coated silica particles is poor, since it contains only carbon and hydrogen atoms, which scatter much less than silicon, being located in the core. Therefore the obtained TEM diameter is at maximum reduced by double the corona thickness, which is about 4nm. Taking that into account we reach about 71nm for the diameter, which gives then a ratio of the different moments of 83/71=1.17, also in fair agreement with the expectation.

C. SANS Experiment

We have performed the SANS experiments at the SANS I machine at the SINQ spallation source at the PSI in Villigen, Switzerland[20]. We used thermal neutrons of wavelength λ=0.8nm having a wavelength spread $\Delta\lambda/\lambda$ of about 0.1. The data analysis was performed using the BERSANS software package[21], which accounts for all necessary corrections due to background, transmission, count rate/dead time ratio, masking and radial averaging of the raw data. A standard water sample was used for calibration to absolute scattering intensities and also to account for a non-uniform detector efficiency[22]. All scattering curves were fitted with theoretical expressions thereby taking the resolution of the spectrometer into account using a procedure described by Pedersen et al.[23]. We have measured at two different detector positions, 18 and 6 meters, which give access to a q-range of $0.02<q/\mathrm{nm}^{-1}<1.2$, where q is the scattering vector, defined as $q=|\mathbf{q}|=\frac{4\pi}{\lambda}\sin\frac{\theta}{2}$, with λ being the neutron wavelength and θ being the scattering angle

III. Results and Discussion

A. Phase Diagram

Our system, octadecyl grafted silica in toluene, was chosen in analogy to octadecane coated silica in benzene, which was described by Verduin and Dhont.[24] and de Kruif et al.[8,9].The main difference between these systems is a shift of the coexistence line with respect to temperature. De Kruif and Schouten[7] have found for the above mentioned silica system in toluene a T_{coex} of about 6°C, whereas we find, that our toluene system phase separates at a lower temperature (T_{coex}= -3°C at ϕ=0.13). We found this T_{coex} by visual observation of the phase behaviour of our colloidal system changing temperature and concentration, as shown in Fig. 3. The difference is probably due to different grafting densities or roughness of the particles on the length scale of the coating layer thickness. In Fig. 3 three different lines are shown: The turbid line, which is a signature of the coexistence line (binodal). Besides the latter thermodynamic information, two other, kinetic items are depicted: First, the viscous line, obtained from the experimental observation, that upon cooling the system towards a temperature, which is below that line leads to a drastic increase of viscosity, but the system still flows, if the tube is tilted. Second, the gel line, which is obtained from the observation, that upon crossing this particular line the system does not flow any more.

We have performed scattering experiments at various volume fractions starting from 0.2% for the determination of the form factor, then 5%, 11.2% 16% and 39.2%. For all these latter volume fractions we observe a structure factor. However, it becomes most pronounced at the highest volume fractions, at 39.2%. A quantitative analysis in terms of a sticky hard sphere structure factor for polydisperse systems has been carried out for different models for the structure factor, which is shown later in the paper. The temperature at which we performed our SANS experiments was about 16°C. From our phase diagram, Fig. 3, it is obvious, that our scattering data at that latter temperature is taken fully in the homogenous phase. This may be completely different for data at higher pressures. De Kruif and Schouten[7] have reported the pressure dependence of the transition temperature at ϕ=0.13 to be dP/dT_{trans}=77bar/K. We have found the same value for our silica/toluene system[25] and thus the vicinity of the turbid line by applying pressures of 1-2kbars at 16°C can easily be reached. We find further, that at a volume fraction of about 15-20%, according to Fig. 3, the gel line seems to intersect the coexistence line. This finding is in agreement with the phase diagram of the related silica/benzene system obtained by Verduin[15] and also in agreement with simulations by Miller and Frenkel[26]. The fact that the gel line intersects the coexistence line is of great practical importance, since it offers the possibility to study the phase transition on a long time scale, probably much longer than it would take without the action of a gelled (percolated or jammed) system.

B. SANS :The form factor for a core-shell particle

We consider the case of a dilute suspension of non-interacting colloidal particles in the absence of multiple scattering and incoherent scattering. “Non-interacting” specifically means that there is no phase coherence between different particles. For details of theory see the general references of Higgins and Benoit[27] and/or Feigin and Svergun[28]. The total macroscopic cross section $d\Sigma/d\Omega(q)$, measured in a SANS experiment, is given by

$$\frac{d\Sigma}{d\Omega}(\mathbf{q}) = N_p F(\mathbf{q})^2 \qquad \text{eq. 1)}$$

where N_p denotes the number density of particles and $F(\mathbf{q})$ the single particle amplitude or form amplitude is defined as:

$$F(\mathbf{q}) \;= \int \left[\rho(\mathbf{r}) - \rho_m\right] \exp(i\mathbf{q}\mathbf{r}) d\mathbf{r} \qquad \text{eq. 2)}$$

ρ_m is the scattering length density of the medium. The form factor $P(q)$ for a spherical object like here is simply given by $P(q) = |F(\mathbf{q})|^2$ and furthermore $q = |\mathbf{q}|$. In the paper by Pedersen[29] many expressions for $P(q)$ for different particle shapes are given. In the case of a sphere with homogeneous scattering length density the expression for the form amplitude reduces to

$$F(q,r) = V(\rho_c - \rho_m) \frac{3[\sin(qr) - qr\cos(qr)]}{(qr)^3} \qquad \text{eq. 3)}$$

We deal with core–shell particles, which consist of an inner core with radius r_c and uniform scattering length density ρ_c .The core is surrounded by a shell of uniform thickness Δr and scattering length density ρ_s. For this model the scattering length density profile is given by:

$$\rho(r) = \begin{cases} \rho_C & \text{for} \quad r \le r_C \\ \rho_S & \text{for} \quad r_C < r < r_C + \Delta r \end{cases} \qquad \text{eq. 4)}$$

Solving eq. 2 for the above scattering density profile yields an expression for the particle form amplitude $F_{cs}(q)$ of a core-shell particle:

$$F_{cs}(q) = (\rho_c - \rho_s)F(q, r_c) + (\rho_s - \rho_m)F(q, r_c + \Delta r) \qquad \text{eq. 5)}$$

$r=r_c+\Delta r$ is the total radius of core plus shell and the $F(q,r)$ is given by eq. 3. The philosophy of eq. 5 is illustrated by the gedanken-experiment, that in order to calculate $F_{cs}(q)$, first the form amplitude of a sphere with ρ_s and radius r is calculated. This is the second term in eq. 5. From that sphere we have to subtract the sphere with radius r_c and ρ_s (the core) and replace it by a sphere with the same radius but a proper ρ_c This is the first term in eq. 5. In a contrast variation experiment, where the scattering length density of the solvent ρ_m is varied, different situations can be obtained: If we chose $\rho_s \approx \rho_m$ (which means, we match out the shell), then the second term in eq. 5 is zero and we observe the form amplitude of the core. On the other hand, if $\rho_c \approx \rho_m$ (we match out the core), then only distribution which describes the form amplitude of the shell remains. This regime is therefore most sensitive for obtaining information on the scattering length distribution within the shell structure. Our colloidal particle system under study is dissolved in toluene, which might be either protonated or deuterated. In table 1 the respective scattering length densities of the constituents are listed. One can see that there is, according to table1, no combination of solvents which will mask out the shell. But since the core can be matched out, the shell alone can be nicely seen. The other extreme in full d-toluene contrast mainly the overall outer dimensions are seen. Since our particles have a size distribution we assumed a Schulz-Zimm distribution for the overall radius $r=r_c+\Delta r$, whereas the corona thickness is supposed to be fixed. This distribution function $L(r)$, which we have to insert in eq. 5 for $r_c+\Delta r$ reads:

$$L(r)=\frac{N}{R_a}\left(\frac{r}{R_a}\right)^{k-1}k^k\exp\left(-k\frac{r}{R_a}\right)\frac{1}{\Gamma(k)}\ \text{with}\ k=\frac{1}{\sigma^2} \qquad \text{eq. 6)}$$

where the normalisation is given by $\int_0^\infty L(r)dr=N$. The variance σ is a measure of the width of the distribution, R_a is a scaling parameter, which defines the maximum of the size distribution for small values of σ and Γ denotes the gamma function. Then the final expression for the determination of the form factor is given by eq. 7, which is equivalent to the coherent macroscopic cross section $d\Sigma/d\Omega(q)_{\mathrm{coh}}$ plus an incoherent macroscopic cross section $d\Sigma/d\Omega_{\mathrm{inc}}$, which does not depend on q. Thus the measured intensity $I(q)$ is given by

$$I(q)=\frac{d\Sigma_{total}}{d\Omega}(q)=\frac{d\Sigma_{coh}}{d\Omega}(q)+\frac{d\Sigma_{inc}}{d\Omega}=N_p\left\langle F_{cs}^2(q)\right\rangle+I_{inc} \qquad \text{eq. 7)}$$

where N_p denotes the number density of particles and I_{inc} is the q-independent background and the $\langle\ldots\rangle$ denote the average over the particle sizes. Eq. 7 is furthermore not valid at higher volume fractions. Then the assumption of no interactions between spheres leading to eq. 1 is no longer valid. At higher concentrations we observe interference between different particles and thus to the development of a structure factor $S(q)$, see the next section III.C.

C.SANS: Systems with structure factor *S*(*q*)

If the assumption that there is no phase coherence between different particles leading to eq.1 is not valid, then we have to extend eq. 1 for these contributions stemming from different particles *i,j*:

$$\frac{d\Sigma}{d\Omega}(\mathbf{q}) = \frac{1}{N_p}\sum_{i,j}^{N_p} F_i(q)F_j^*(q) \times \exp\left[i\mathbf{q}\mathbf{r}_{ij}\right] \qquad \text{eq. 8)}$$

Here the *F*'s are the scattering amplitudes of particles *i* and *j*.

$$\frac{d\Sigma}{d\Omega}(\mathbf{q}) = \sum_{i}^{N_p} F_i^2(q) + \frac{1}{N_p}\sum_{i\neq j}^{N_p} F_i(q)F_j^*(q) \times \exp\left[i\mathbf{q}\mathbf{r}_{ij}\right] \qquad \text{eq. 9)}$$

where the first term is the scattering intensity of non-interacting particles (limit of dilute system). The second term describes the interference effects between different particles. In case that the particle size is independent of the particle position we can separate the averaging over the form factors from the averaging over the positions (decoupling approach)

$$\begin{aligned}\frac{d\Sigma}{d\Omega}(q) &= N_p\left\langle F^2(q)\right\rangle + \frac{1}{N_p}\left\langle F(q)\right\rangle^2 \sum_{i\neq j}^{N_p} \exp\left[i\mathbf{q}\mathbf{r}_{ij}\right] \\ &= N_p\left\langle F^2(q)\right\rangle + N_p\left\langle F(q)\right\rangle^2\left[S(q)-1\right]\end{aligned} \qquad \text{eq. 10)}$$

where *S*(*q*) is the structure factor for radial symmetric interactions. It depends only on the arrangement or positions of the particles. That in turn reflects the interaction potential between particles. For some interaction potentials like i.e. sticky hard spheres $S(q)$ can be obtained analytically. For a dilute system the structure factor is identical to one and hence eq. 7 follows from eq. 10 (except I_{inc}). There is a fundamental problem involved in the experimental determination of $S(q)$. Strictly spoken $S(q)$ can only be determined, if the two averages $\left\langle F^2(q)\right\rangle$ and $\left\langle F(q)\right\rangle^2$ are the same, which is normally not the case. An exception would be a solution of identical spherical symmetric particles. However, in our case we are always faced with a size distribution and therefore the two averages are not identical. Thus to obtain the effective structure factor $\tilde{S}(q)$, the concentrated system is measured and is divided by the dilute case and normalized with the concentration

$$\tilde{S}(q)=\frac{I(q)_{conc}}{I(q)_{dilute}}=1+\frac{\left\langle F(q)\right\rangle^2}{\left\langle F^2(q)\right\rangle}\left[S(q)-1\right]\xrightarrow{mono.,ident.}S(q) \qquad \text{eq. 11)}$$

The above described decoupling approach assumes, that the interaction potential and therefore also the structure factor $S(q)$ is the same for all pairs of particles, independent of their size. However, this is only a sufficient good approximation, when the size distribution is very narrow. Several approaches have been suggested (see ref. 29 and references in there) to take also different interaction potentials between particles of different size into account. A rigorous treatment of the problem is described by Vrij[30] for polydisperse hard spheres, which has been extended to polydisperse sticky hard spheres by Robertus et al.[16] A numerically more simple to implement approach (scaling approximation) has been suggested by Gazillo and Giacometti[31,32]. We have tested all three approaches to our data set. It turned out that for below 5% all three approximations yield sufficiently good results. For higher concentrations it is, however, necessary to use either the rigorous approach from Vrij or the one from Gazzillo et al., which gives almost the same result. In Fig. 4 we have compared all approaches with each other to our experimental data obtained at the highest concentration and at a scattering length density of the solvent of ρ=2.07x10^{10} cm^{-2} .We find that, except for the scaling approximation and the exact solution, all other approximations show deficiencies either in the intensity at low q and/or value for the first maximum and the width of the peak. The data shown in Fig. 4 were taken at a contrast slightly off the match point, since we had to adjust the scattered intensity to avoid multiple scattering. We are, however, interested in the behaviour of our system at the match point, since there we expect to be most sensitive on changes in the corona. In order to find out how the structure factor of the system at high concentrations depends on the scattering length densities of the solvent around the zero average contrast condition, we have calculated the structure factor on the basis of the Robertus model[16] for different values of ρ_{sol}. This is shown in Fig. 5, where the parameters used are given in the figure. Clearly we observe a strong increase of intensity for low q around the match point (about 2.15x10^{10}cm^{-2}), which means that $\tilde{S}(q)$ depends strongly on the zero contrast condition. Obviously we observe shape fluctuations, since at zero contrast we are very sensitive on small deviations from the match point condition. This q-dependence is thus an effect of an inhomogeneous particle in combination with a size distribution. It also means that it is difficult to analyse data around zero average contrast in terms of $I(q\rightarrow 0)$ and stickiness, because that also would lead to an increase of intensity for low q. Therefore, determining the effective structure factor close to the match point, is very sensitive to small errors in the scattering length density. As the analysis on the level of form factors and structure factors separately seems to be artificial anyway, we will in the next section present the results of the contrast variation on the basis of the total intensity $I(q)$ and not on the structure and form factor separately. We take structure factor effects into account using the Robertus approach[16] and the form factor from the model for the core–shell particle, eq.5.

D. SANS: The contrast variation

Our particles are core shell particles, where the respective scattering densities ρ of the core, shell and surrounding solvent are given in table 1. We have performed most of our experiments by measuring $I(q)$ of our silica particles at a concentration of 5% in a mixture of h-and d-toluene around zero average contrast, in order to find a compromise between sufficient intensity on the one hand and not too large influence of a structure factor on the other hand. According to table 1, there is no combination of solvents, which will mask out the shell. But since the core can be matched out, the shell alone can be nicely seen. A contrast variation experiment has been carried out to get a more detailed picture of the inner structure of the colloid, especially about the shell, i.e. about its thickness and also about the amount of solvent in it. The contrast variation has been performed at a scattering length densities of the solvent ranging from $1.8\text{x}10^{10}\text{cm}^{-2}$ to $2.5\text{x}10^{10}\text{cm}^{-2}$ in incremental steps of $0.1\text{x}10^{10}\text{cm}^{-2}$. In a first attempt each curve was fitted with eq. 7 in combination with eq.10, where we have fixed the width of the size distribution to σ=0.124 and the shell thickness to Δr=2nm. The results for the so obtained scattering length densities for the core and shell are shown in Fig. 6.

From Fig. 6 several important conclusions can be drawn: First of all the so obtained core scattering length density as a function of the scattering contrast is a linear function of the scattering length density of the mixed solvent we used. Moreover the slope is –1, which indicates strongly, that the core is not interpenetrated by solvent molecules. Further evidence comes from the scattering length density of the solvent for which the scattering contrast of the core is zero. This gives a value for ρ_{silica} of $2.4\text{x}10^{10}\text{cm}^{-2}$ which can be compared to calculations from its chemical composition. The nominal density of silica is ρ_p=2.2g/cm^3. It is known, however, that Stöber silica particles contain water and ethanol, which in turn decreases the particle density ρ_p. Here values ranging from ρ_p=(1.8±0.1)g/cm^3 to ρ_p=(2.0±0.05)g/cm^3 have been reported[33,34], in agreement with our density value. Using therefore the reasonable assumption, that our Stöber particles are well described by a chemical composition like $(SiO_2)_6H_2O$[35], with a mean density of ρ_p=1.9g/cm^3, yields a scattering length density of ρ=2.81x10^{10}cm^{-2}. An addition of 3% ethoxy groups, which is thought to be reasonable[35], decreases the scattering length to ρ=2.7x10^{10}cm^{-2}. Still from our fit, cf. Fig. 6, we get a value of ρ_{silica}=2.4x10^{10}cm^{-2}. The so obtained value is significantly smaller (about 11%), than the calculated one for the (scattering length) density of silica. On the other hand the slope of -1 confirms that the core is not solvent interpenetrated.

The results for the scattering length density for the shell scatter more, mainly due to the fact, that the shell is rather thin as compared to the diameter of the particle and hence its characterisation is more difficult. Moreover a rather unphysical independence of the scattering contrast on the scattering length of the solvent was found. This becomes even more evident, if we add the value for the contrast of the pure octadecane layer (ρ=-0.234x10^{10}cm^{-2}) to the plot at zero solvent, which acts as a constraint in performing a linear fit to the shell contrast fit values. Then the fit yields a reasonable linear dependence with a slope of –0.61, which indicates penetration of the layer by solvent molecules. The degree of penetration can be estimated by assuming a linear dependence of the shell scattering length density with ϕ_{sol}, the volume fraction of solvent in the shell. Accordingly we write:

$$\rho_{shell} = \phi_{sol}\rho_m + (1-\phi_{sol})\rho_s \qquad \text{eq. 12)}$$

For this particular case, assuming the shell thickness to be 2nm, a mean ϕ_{sol} of 0.4 is obtained.

In summary we conclude, that the single curve fitting yields rather difficult to interpret results, since it needs to fix parameters, in order to get the fits to converge. We have carefully checked whether keeping various parameters fix (solvent penetration and Δr not obtainable separately with confidence) will change the results such that a more physical picture emerges, but that was not the case. Therefore we decided to develop a program in order to be able to handle all the different constrains and also to get a coherent result for the description of the scattering intensities. The program can fit simultaneously all data sets with a global set of parameters. This allows us to separate the influence of several parameters on the intensity signal, which would otherwise be strongly correlated parameters. In the so called global fitting routine, we used as free parameters in the fit only r_c, σ_c, Δr, ρ_c and ϕ_{sol} according to eqs. 7 and 12. The scattering length density of octadecane ρ_s was kept fixed for each global run to ρ_s=–0.234x10^{10}cm^{-2}. The data at 5% in volume fraction were fitted with regard to $S(q)$ assuming a decoupling approach using a fixed hard sphere radius of r=35nm. Fig. 7a,b shows the results of the global fit and the parameters are listed in table 2.

At this point we refer back to Fig. 5, where we had calculated the Robertus structure factor[16] for different values of the solvent scattering length density around zero contrast. There we found a strong increase of $S(q)$ at zero contrast, being about ρ_m=2.15x10^{10}cm^{-2}. From the inspection of our experimental data in Fig. 7a we find the match point at about 2.1-2.2x10^{10}cm^{-2} , in agreement with that former finding. The intensity $I(q)$ decreases for small q at zero contrast, although $S(q)$ increases, cf. Fig. 5. The reason is that the form factor for a core-shell particle at zero contrast decreases stronger for small q, so that the intensity drops. We had seen that the contrast variation in combination with a single curve fitting was not able to allow a separate determination of the amount of solvent in the shell and the shell thickness (cf. Fig. 6). Now we carried out the global fitting for several values of the shell thickness. It has been found, that as long as the product of (1-ϕ_{sol}) times the volume of the shell V_{shell} was kept constant, the resulting scattering curve did not change significantly. Hence V_{shell}(1-ϕ_{sol})=const. or equivalently Δr(1-ϕ_{sol}) =const. (for Δr<<r_c) gives a hyperbolic relation between Δr and ϕ_{sol}. To proof this, we performed a fit for several fixed values of the shell thicknesses and plotted the amount of solvent ϕ_{sol} as a function of the shell thickness. The result is shown in Fig. 8 together with the χ^2 value of the fit. The plot shows, that practically without a loss in the fit quality we always could adjust the amount of solvent, when we changed the value of the shell thickness in the fit such that $V_{shell}(1-\phi_{sol})$=const.. Furthermore the global fit supports the results from the single curve fitting, cf. Fig. 8, as it shows, that for a Δr of 2nm indeed ϕ_{sol} is about 0.4, cf. Fig. 8. However, without global fit this result would have been thought to be obtained by chance. Moreover, the important relation between volume and $(1-\phi_{sol})$ would not have been established. To distinguish between the influences of these two parameters, one needs to measure the coherent scattering intensity at large scattering vectors q to determine Δr, which is not possible, because the measured intensity for large q is dominated by the incoherent background of the sample. It can be shown, that based on bond length calculations that a C_{18} alkyl chain has in the stretched configuration a length of about 2.3nm. This value corresponds roughly to the minimum of χ^2 as shown in Fig.8 and corresponds thus to a solvent penetration of 50% not too far from the value of 40% as obtained from single curve fitting.

Another important information, which can be obtained from Fig. 8 is given by the value of the shell volume when there is no solvent in it. That value is proportional to the shell thickness under conditions of no penetration and amounts to 1.25nm. Given the core diameter distribution, the total amount of octadecyl chains in the shell of the particles as obtained from SANS is 10.3% by volume. By elemental analysis on dried particles, however, a total volume fraction of alkyl chains of 24.3% was determined. This finding is supported by comparing the Raman region around 3000cm^{-1} of a concentrated silica suspension in toluene with a dilution series of octadecane in toluene from about 70wt% down to 5wt%. From an integration of the band intensities in that particular wave number regime we could estimate the amount of methyl(ene) groups to be in the order of 8-10 wt%, which corresponds to a similar volume of alkyl chains as from elemental analysis. Because it is not possible to obtain a good global fit of the SANS data with a much different amount of octadecyl chains in the shell, the only explanation seems to be that the remaining amount of alkyl chains of 14% by volume is located in the core of the particles. This can be checked by calculating ρ_c for this composition and comparing it to the value obtained from the fit of the SANS data. If we calculate ρ_c for a core composed of 15.6% alkyl chains (15.6% alkyl chains in the core corresponds to 14% of the complete particle) and 84.4% of silica with a composition of $6(SiO_2)H_2O$[35]and a density of 2.0 g/mL, we obtain ρ_c=2.45×10^{10} cm^{-2}. Indeed, this is in excellent agreement with the ρ_c of 2.41×10^{10} cm^{-2} as obtained from the SANS analysis, giving a strong indication, that some organic material is contained throughout the silica core. These alkyl chains in the core are thought to be ethoxy groups from the Stöber synthesis or the start of the grafting procedure, or octadecyl chains entering the core during the grafting at 190-200°C. These results on the grafting density also agree with the resent estimate of the grafting density of ~1/3 octadecyl chains and 2/3 solvent for octadecyl grafted silica particles in hexadecane as studied with the non-linear optical technique vibrational sum frequency scattering[36]. As elemental analysis of this type of colloidal particles often results in grafting densities of around 100%[18] , it seems likely that these particles generally contain a significant amount of organic material in the core.

We have further used the values for r_c, Δr and standard deviation σ from the global fit to calculate the distribution function according to eq. 6 and compare this result with the distribution obtained by TEM, as shown in Fig. 2. The result of this calculation is shown in Fig. 9. Two distributions are shown, the size distribution of the total radius $L(r_c+\Delta r)$ and the size distribution of the core $L(r_c)$ alone, which is simply shifted by Δr=2.3nm, since it is not clear, to what extent the shell is seen in the TEM. Although the TEM distribution is somewhat more skewed than the Schulz-Zimm distribution used in the SANS fit, the results of the two methods are in good agreement.

IV. Conclusions

In this paper we have employed SANS on a core-shell particle with a rather thin shell ($r_c/\Delta r \approx 14$). We analysed the shell thickness and penetration of the shell by solvent molecules in terms of a contrast match experiment and found that only by a refined global fit routine reasonable parameters characterizing the system could be obtained. Thereby one fits simultaneously all data sets with a global set of parameters, which allows to separate the influence of several strongly correlated parameters on the intensity signal. In that way we were able to obtain the thickness of the shell, the core radius, the distribution of the core radii, the core contrast and the penetration of the shell by solvent, cf.table2. With regard to shell properties, we found that only the product $V_{shell}(1-\phi_{sol})$ could be determined with high accuracy, whereas the determination of the shell thickness or the penetration of solvent separately is less accurate. By chemical and spectroscopic means we could furthermore estimate the dry shell volume separately, from which in combination with the SANS results we could conclude that a significant amount of alkyl groups must be contained in the core. We further found that the core-shell particle shows a strong q-dependence of $\tilde{S}(q)$ at zero contrast conditions. The $\tilde{S}(q)$ increases the more we are approaching to zero contrast. This stems from a non-uniform scattering length density profile and a distribution of radii. With regard to the analytical expression for $\tilde{S}(q)$ we found, that the description by Robertus et al.[16] is most adequate and likewise the ansatz by Gazzillo et al.[31,32] based on a scaling approximation.. The often used decoupling approach works reasonably well only up to volume fractions of about 0.05 at zero average contrast.

References:

1. A. Vrij and R. Tuinier; *Structure of Concentrated Colloidal Dispersions* in: Fundamentals of Interface and Colloid Science, Vol. IV: Colloids. J. Lyklema (ed.), Elsevier, (2005)
2. E. A. Nieuwenhuis, C. Pathmamanoharan and A. Vrij; *J. Coll. Interface Sci*, **81**, 196 (1981)
3. R. J. Baxter; *J. Chem. Phys*., **49**, 2770 (1968)
4. J. W. Jansen, C. G. De Kruif and A. Vrij; *J. Colloid Interface Sci*.,**114**, 471 (1986)
5. J. Edwards, D. H. Everett, T. O'Sullivan, I. Pengalon and B. Vincent; *J. Chem. Soc., Faraday Trans. 1*, **80**, 2599 (1984)
6. P. W. Rouw and C. G. de Kruif; *J. Chem. Phys*.,**88**, 7799 (1988)
7. C. G. De Kruif and J. A. Schouten; *J. Chem. Phys*.,**92**, 6098 (1990)
8. C. G. De Kruif, W. J. Briels, R. P. May and A. Vrij; *Langmuir*, **4**, 668 (1988)
9. C. G. De Kruif, P. W. Rouw, W. J. Briels, M. H. G. Duits, A. Vrij and R. P. May; *Langmuir,* **5**, 422 (1989)
10. H. Verduin; *PhD Thesis*, University of Utrecht, (1996)
11. M. Zackrisson, A. Stradner, P. Schurtenberger and J. Bergenholtz; *Langmuir*, **21**, 10835 (2005)
12. A. Rübe, G. Hause, K. Mäder and J. Kohlbrecher; *J. of Controlled Release*, **107**, 244 (2005)
13. N. Dingenouts, S. Seelenmeyer, I. Deike, S. Rosenfeld, M. Ballauff, P. Lindner and T. Narayanan; *Phys. Chem. Chem. Phys*., **3**, 1169 (2001)
14. J. Wagner*; J. Appl. Cryst*. ,**37**, 750 (2004)

15. T. Riley, C. R. Heald, S. Stolnik, M. C. Garnett, L. Illum, S. S. Davis, S. M. King, R. K. Heenan, S. C. Purkiss, R. J. Barlow, P. R. Gellert and C. Washington; *Langmuir*, **19**, 8428 (2003)
16. C. Robertus, W. H. Philipse, J. G. H. Joosten and Y. K. Levine; *J. Chem. Phys*., **90**, 4482 (1989)
17. W. Stöber, A. Fink and E. Bohn*; J. Colloid Interface Sci*., **26**, 62 (1968)
18. A. K. van Helden, J. W. Jansen and A. Vrij*; J. Colloid Interface Sci*., **81**, 354 (1981)
19. J. C. Thomas; *J. Colloid Interface Sci*.; **117**, 187 (1986)
20. J. Kohlbrecher and W. Wagner*, J*. Appl. Cryst. **33**, 804 (2000)
21. U. Keiderling, *Appl. Phys. A* **74**, S1455 (2002)
22. P. Strunz, J. Saroun, U. Keiderling, A. Wiedenmann and R. Przenioslo; *J. Appl. Cryst*., **33**, 829 (2000)
23. J. S. Pedersen, D. Posselt and K. Mortensen; *J. Appl. Cryst*., **23**, 321 (1990)
24. H.Verduin and J. K. G. Dhont; *J. Colloid Interface Sci*., **172**, 425 (1995)
25. J. Buitenhuis, J. Kohlbrecher, M. P. Lettinga and G. Meier; to be published
26. M. A. Miller and D. Frenkel; *Phys. Rev. Lett*. **90**, 135702 (2003))
27. J. S. Higgins and H. C. Benoit; *Polymers and Neutron Scattering*, Oxford Science Pub., (1994)
28. L. A. Feigin and D. I. Svergun; *Structure Analysis by Small-Angle X-Ray and Neutron Scattering,* Plenum Press, (1987)
29. J. S. Pedersen; *Adv. Colloid Interface Sci*., **70**, 171 (1997)
30. A.Vrij; *J. Colloid Interface Sci*., **90**,110 (1982)
31. D. Gazzillo, A. Giacometti, R. G. D. Valle, E. Venuti and F. Carsughi;*J. Chem. Phys*., **111**, 7636 (1999)
32. D. Gazzillo and A. Giacometti; *Physica A*, **304**, 202 (2002)
33. A. A. Chabanov, Y. Jun and A. J. Norris; *Appl. Phys. Lett*., **84**, 3573 (2004)

34. B. J. Maranzano and N. J. Wagner; *J. Chem. Phys.*,**114**, 10514 (2001)

35. A. van Blaaderen and A. Vrij ; *Synthesis and Characterization of Colloidal Model Particles Made from Organoalkoxysilanes*" in: The Colloid Chemistry of Silica, Advances in Chemistry Series No. 234; H.E. Bergna (ed.)ACS, (1994).

36. S. Roke, J. Buitenhuis, J. C. van Miltenburg, M. Bonn and A. van Bladeren; *J. Phys.: Condens. Matter*, **117**, S3469 (2005)

Tables:

Compound	ρ in 10^{10} cm^{-2}
toluene-d8	5.66
Silica	≈2.4 (found experimentally) (2.7 theoretical value)
toluene-h8	0.94
Octadecane	-0.23

Table 1

r_c /nm	σ_c	Δr/nm	$\rho_c/10^{10}$cm^{-2}	ϕ_{sol}
32.3	0.124	2.3	2.393	0.503

Table 2

Table Captions

Table 1: Values of the coherent scattering length densities ρ in 10^{10}cm^{-2} for all involved compounds. As can be seen, it is possible to contrast match the silica core by a proper mixture of deuterated and protonated toluene. The scattering length density of the corona is negative and can not be matched by any combination of the two toluenes. The value for silica depends on its density, water and ethanol content and is thus not exactly known.

Table 2: Parameters of global fit

Figure Captions

Figure 1: Pair interaction V(r) between two adhesive hard spheres with diameter σ and a square well with width Δ and depth ε

Figure 2: Size distribution as obtained from a TEM analysis of 177 silica particles.

Figure 3: Phase diagram of silica spheres coated with octadecane in toluene. Lines are guide to the eye.

Figure 4: Comparison of experimental data (black squares) obtained by SANS from a colloid solution with volume fraction ϕ=0.392 and at a scattering length density of the solvent of ρ=2.07x10^{10} cm^{-2} with different models for the structure factor (as listed in the inset) using a polydisperse core-shell form factor, as given by eq.5. Only the scaling approximation and the exact solution describe the data well.

Figure 5: Calculation of $\tilde{S}(q)$ for parameters as given in the figure at a volume fraction ϕ=0.392 (upper right inset, from global fit, see Fig. 7) using the Robertus model[16] for the structure factor calculated for different scattering length densities of the solvent as indicated on the left. The large increase of $\tilde{S}(q)$ at low q is most pronounced at zero contrast conditions.

Figure 6: Plot of the scattering contrasts (circles for core and squares for corona) obtained from single curve fitting of the 5% data with eq.7, with a fixed size distribution σ=0.124 and

fixed shell thickness of Δr=2nm versus scattering length densities of the solvent. $S(q)$ was taken into account on the basis of the decoupling approach (eq. 10) using r_c=33.6nm, ρ_c=2.7x10^{10}cm^{-2} and ρ_s=-0.234x10^{10}cm^{-2}.

Figure 7a: Fit of eqs. 6 and 7 and structure factor according to eq.10 to the experimental data points obtained by SANS from a 5% solution at various contrasts around the match point of the core scattering length density as indicated in the upper right inset. Around ρ=2.1-2.2x10^{10}cm^{-2} the match point is obtained (lowest intensity for vanishing q) which highlights the form factor of a hollow sphere.

Figure 7b: Fit of eqs. 6 and 7 to the experimental data points obtained by SANS from a 0.2 % solution of coated silica spheres in d-toluene(top curve, which reaches for high q the lowest intensity, because it is measured in pure d-toluene) and fit of eqs. 6 and 7 and structure factor according to Robertus et al.[16] to three higher volume fractions, where the development of the structure factor can be observed. In the inset the volume fractions and scattering length densities of the solvent are listed. The latter three curves reach for high q a kind of plateau, which stems from the incoherent scattering from a part of the solvent, h-toluene.

Figure 8: Correlation between shell thickness and amount of solvent in the shell. The product of $V_{shell}(1-\phi_{sol})$=const. and thus a hyperbolic dependence between Δr and ϕ_{sol} is expected. Open symbols are results from global fit, full line is expected hyperbolic dependence. Also shown as full symbols is the quality of the fit. The best fit is obtained for shell thicknesses around 2.3nm.

Figure 9: The size distribution as obtained from the global fit of the SANS results compared to the size distribution as obtained by TEM.

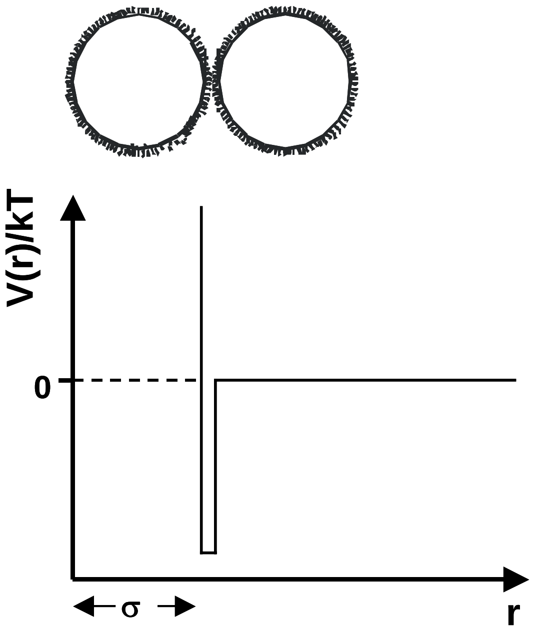

Figure 1

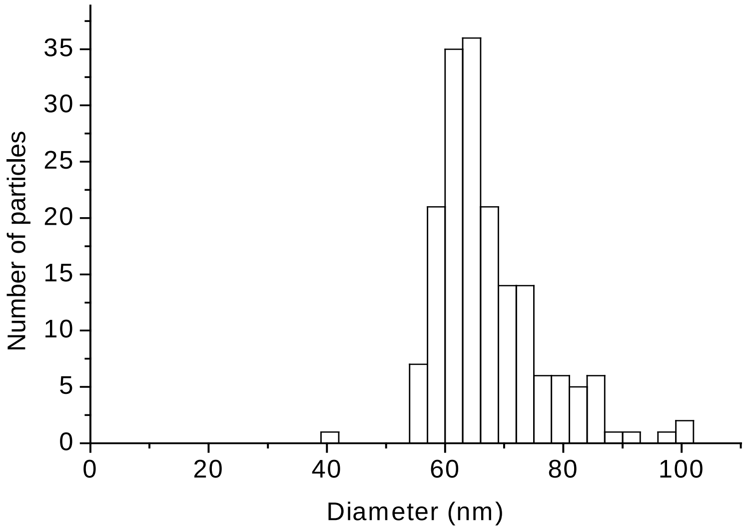
Number of particles
0
5
10
15
20
25
30
35
0
20
40
60
80
100
Diameter (nm)

Figure 2

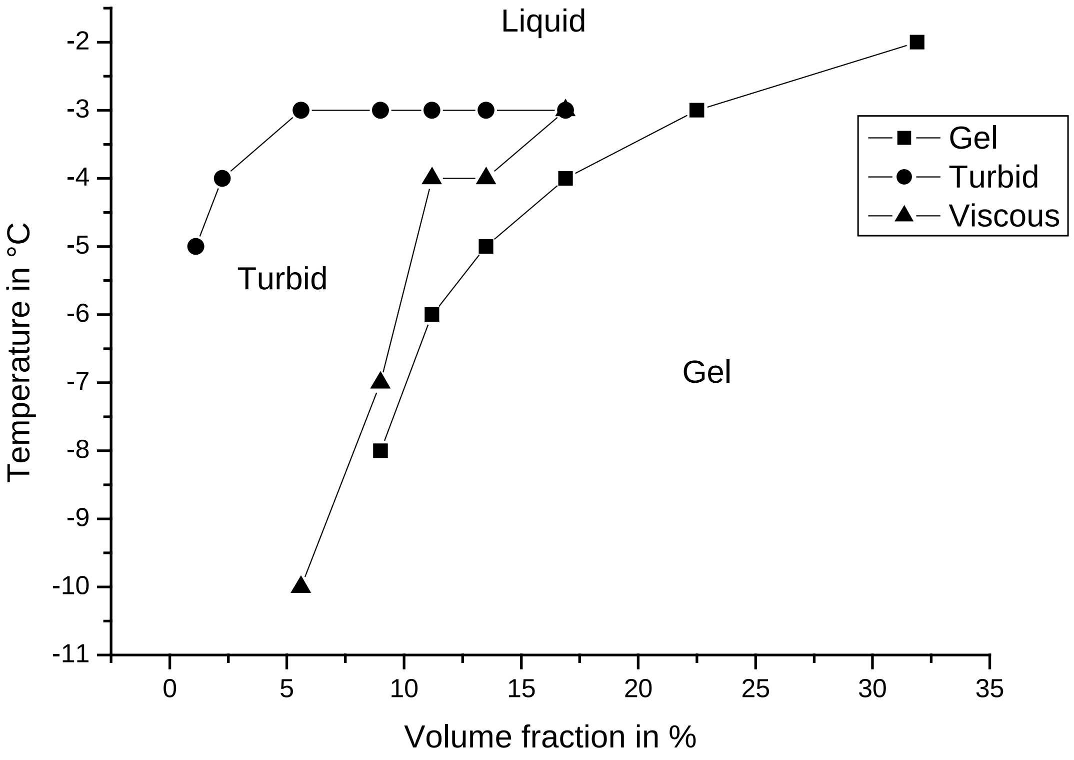
Liquid
Turbid
Gel
■ Gel
● Turbid
▲ Viscous
Temperature in °C
-2
-3
-4
-5
-6
-7
-8
-9
-10
-11
0
5
10
15
20
25
30
35
Volume fraction in %

Figure 3

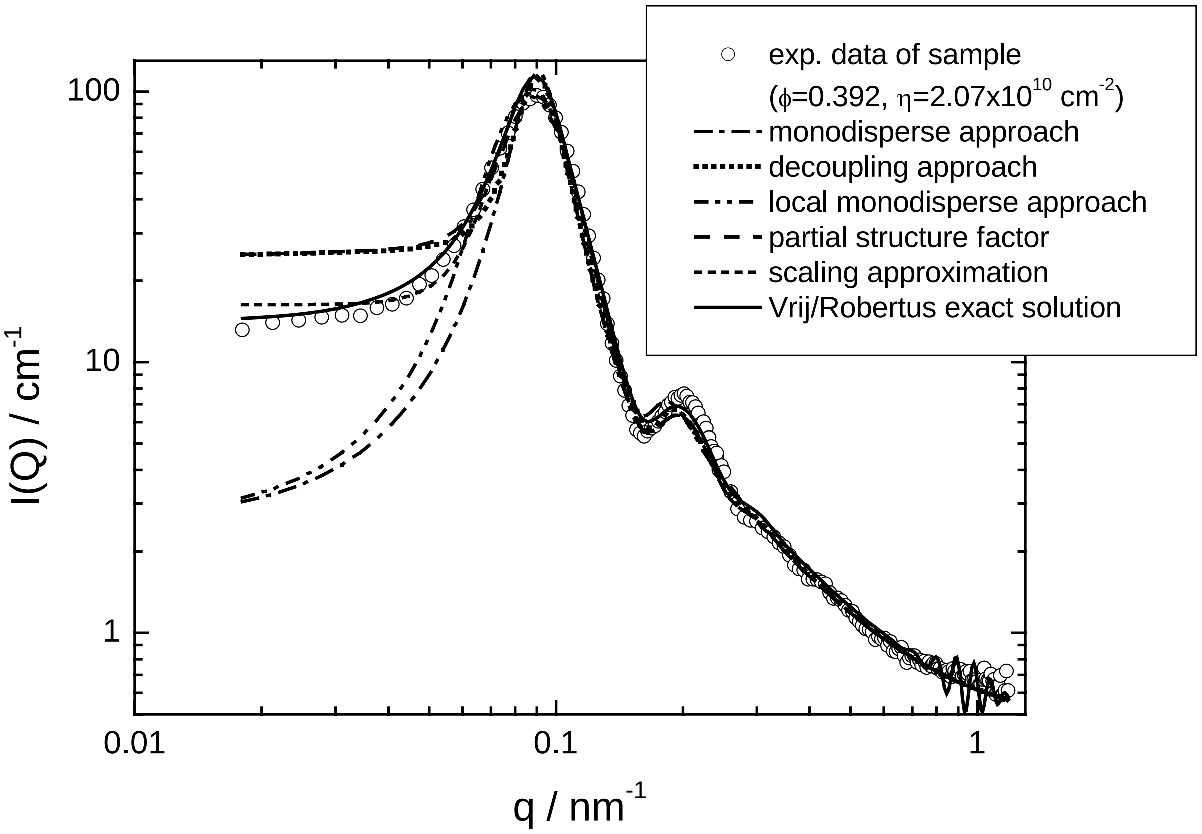

I(Q) / cm^{-1}
q / nm^{-1}
100
10
1
0.01
0.1
1
exp. data of sample
(ϕ=0.392, η=2.07x10^{10} cm^{-2})
monodisperse approach
decoupling approach
local monodisperse approach
partial structure factor
scaling approximation
Vrij/Robertus exact solution

Figure 4

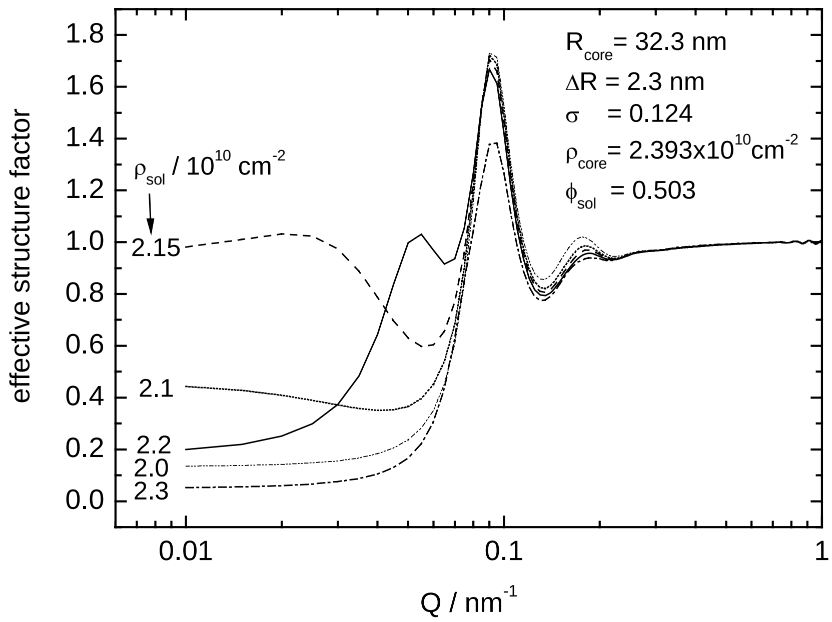

effective structure factor
Q / nm^{-1}
0.0
0.2
0.4
0.6
0.8
1.0
1.2
1.4
1.6
1.8
0.01
0.1
1
ρ_{sol} / 10^{10} cm^{-2}
2.15
2.1
2.2
2.0
2.3
R_{core}= 32.3 nm
ΔR = 2.3 nm
σ = 0.124
ρ_{core}= 2.393x10^{10}cm^{-2}
ϕ_{sol} = 0.503

Figure 5

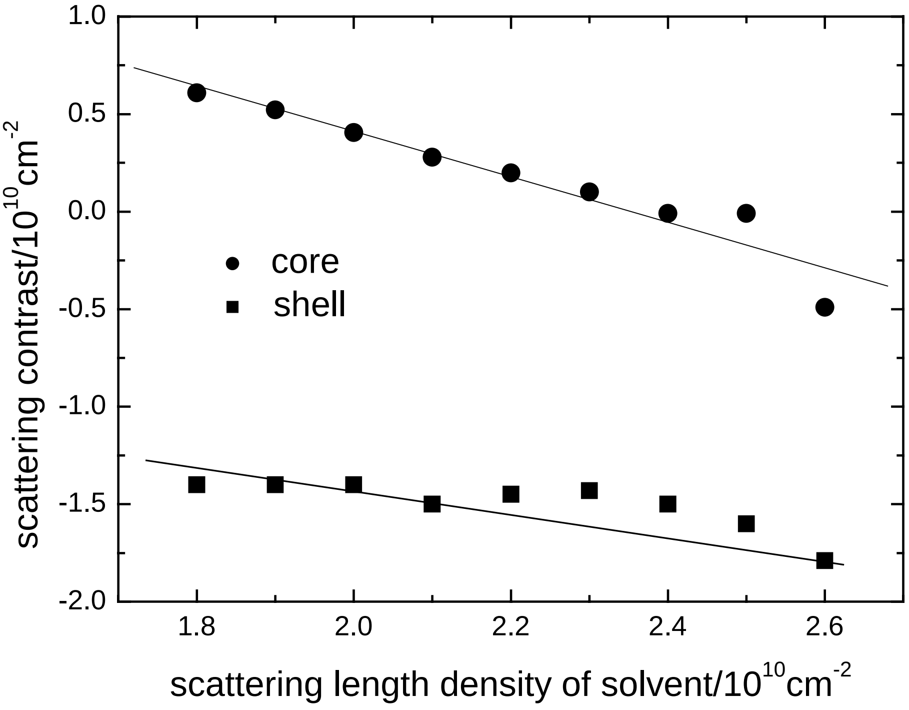
1.0
0.5
0.0
-0.5
-1.0
-1.5
-2.0
1.8
2.0
2.2
2.4
2.6
scattering contrast/10^{10}cm^{-2}
scattering length density of solvent/10^{10}cm^{-2}
● core
■ shell

Figure 6

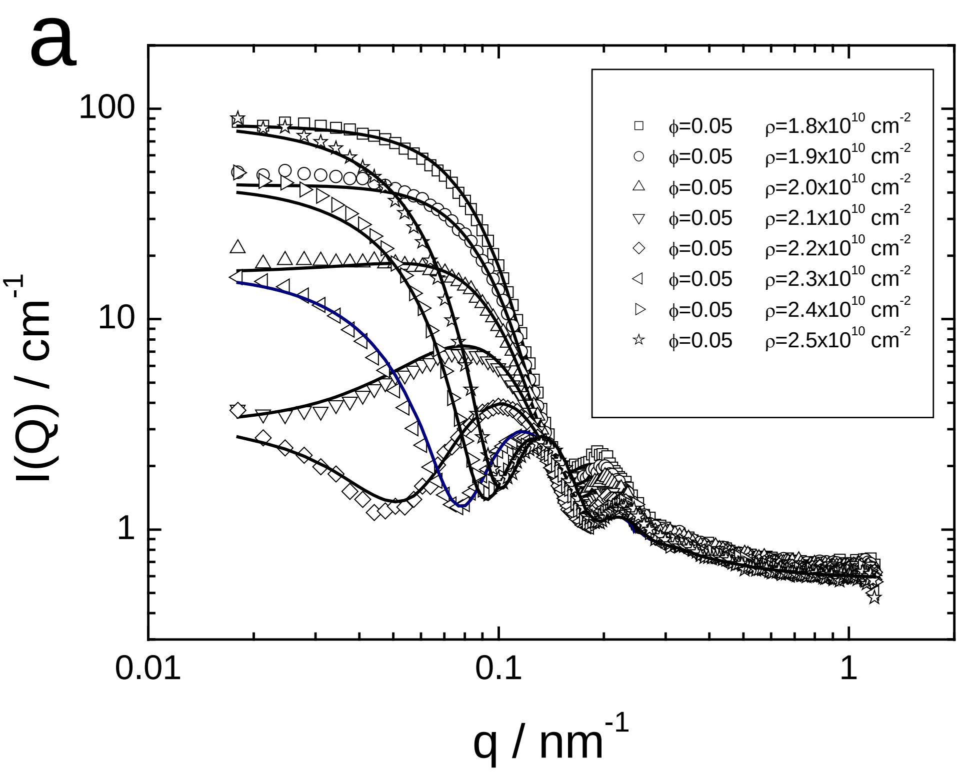
a
100
10
1
0.01
0.1
1
I(Q) / cm^{-1}
q / nm^{-1}
□ ϕ=0.05 ρ=1.8x10^{10} cm^{-2}
○ ϕ=0.05 ρ=1.9x10^{10} cm^{-2}
△ ϕ=0.05 ρ=2.0x10^{10} cm^{-2}
▽ ϕ=0.05 ρ=2.1x10^{10} cm^{-2}
◇ ϕ=0.05 ρ=2.2x10^{10} cm^{-2}
◁ ϕ=0.05 ρ=2.3x10^{10} cm^{-2}
▷ ϕ=0.05 ρ=2.4x10^{10} cm^{-2}
☆ ϕ=0.05 ρ=2.5x10^{10} cm^{-2}

Figure 7a

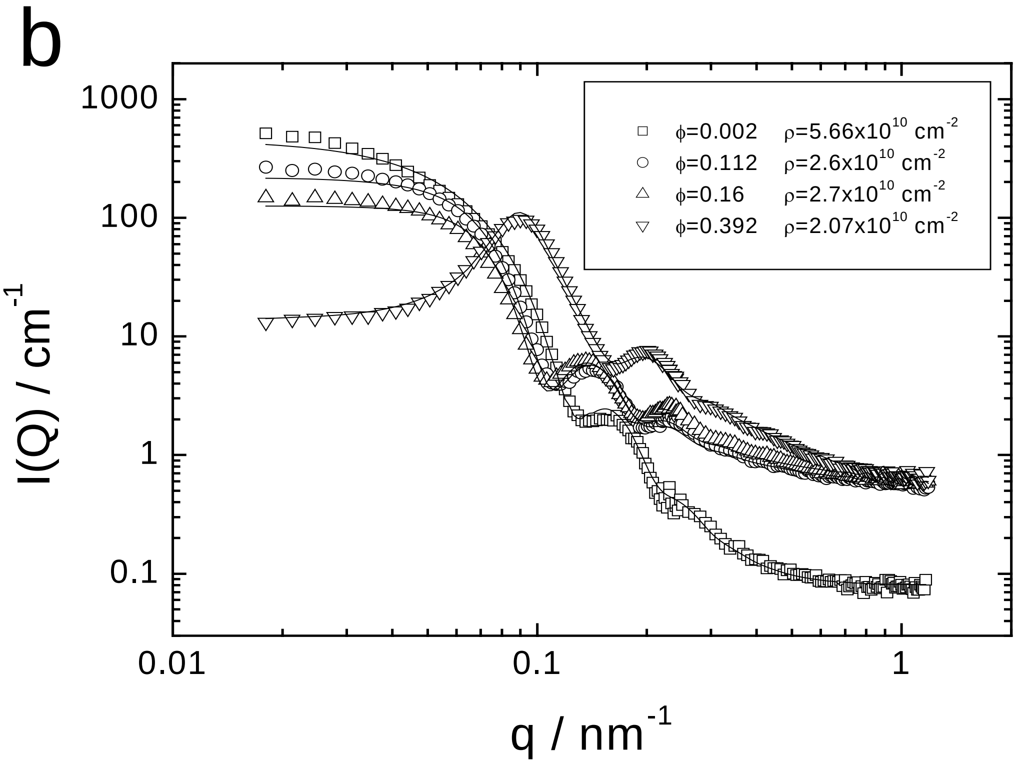
b
1000
100
10
1
0.1
0.01
0.1
1
I(Q) / cm^{-1}
q / nm^{-1}
□ ϕ=0.002 ρ=5.66x10^{10} cm^{-2}
○ ϕ=0.112 ρ=2.6x10^{10} cm^{-2}
△ ϕ=0.16 ρ=2.7x10^{10} cm^{-2}
▽ ϕ=0.392 ρ=2.07x10^{10} cm^{-2}

Figure 7b

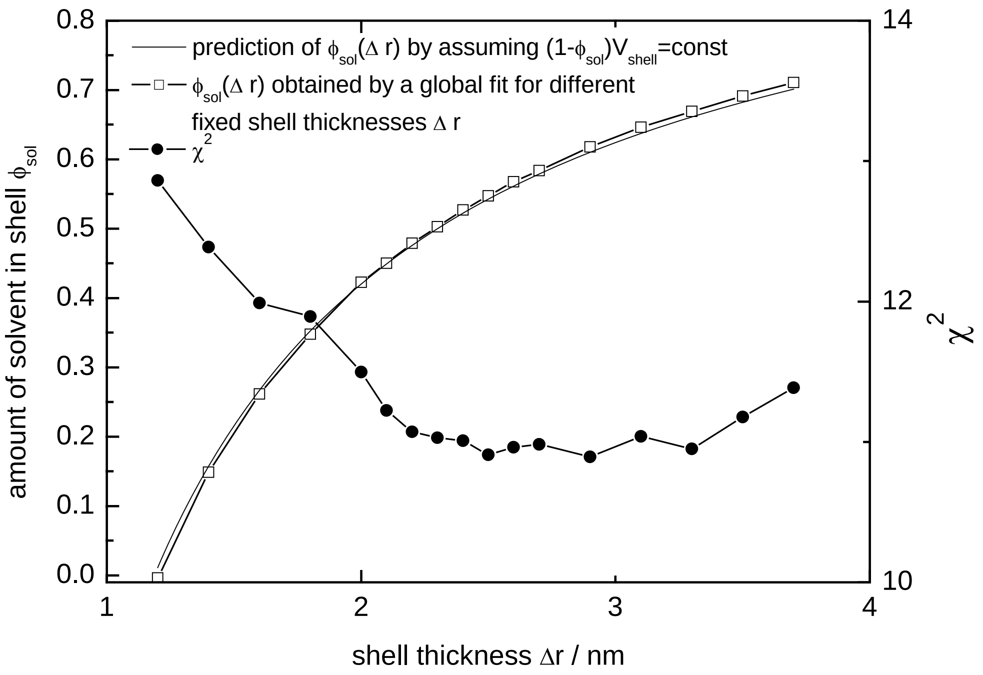
prediction of ϕsol(Δ r) by assuming (1-ϕsol)Vshell=const
ϕsol(Δ r) obtained by a global fit for different fixed shell thicknesses Δ r
χ2
amount of solvent in shell ϕsol
0.8
0.7
0.6
0.5
0.4
0.3
0.2
0.1
0.0
χ2
14
12
10
1
2
3
4
shell thickness Δr / nm

Figure 8

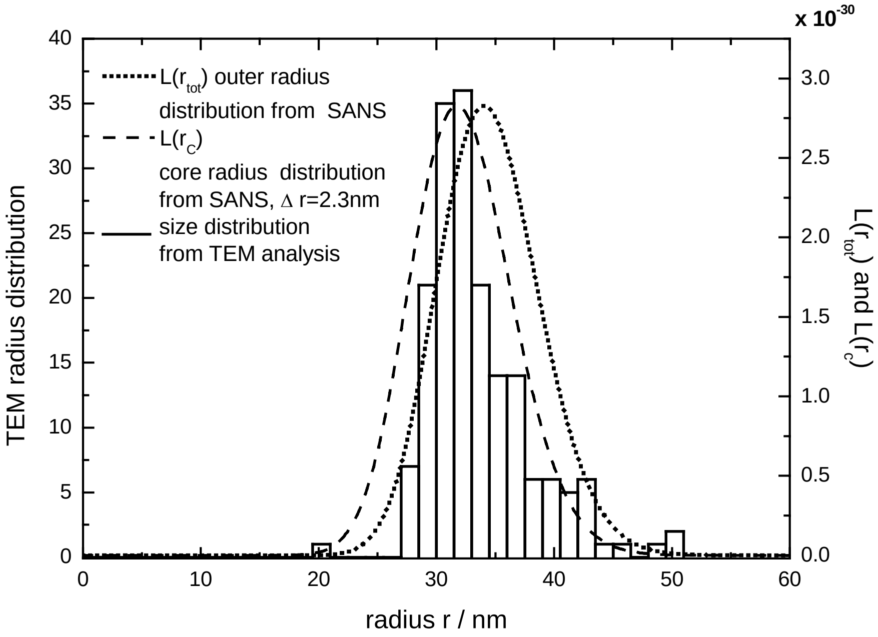

x 10^-30
40
35
30
25
20
15
10
5
0
3.0
2.5
2.0
1.5
1.0
0.5
0.0
0
10
20
30
40
50
60
TEM radius distribution
L(r_tot) and L(r_c)
radius r / nm
L(r_tot) outer radius distribution from SANS
L(r_C) core radius distribution from SANS, Δ r=2.3nm
size distribution from TEM analysis

Figure 9